Supramolecular polymer materials for biomedical applications and diagnostics

Noteborn, W.E.M.

CHAPTER 2

Grafting from a hybrid DNA-dextran graft copolymer by the hybridization chain reaction

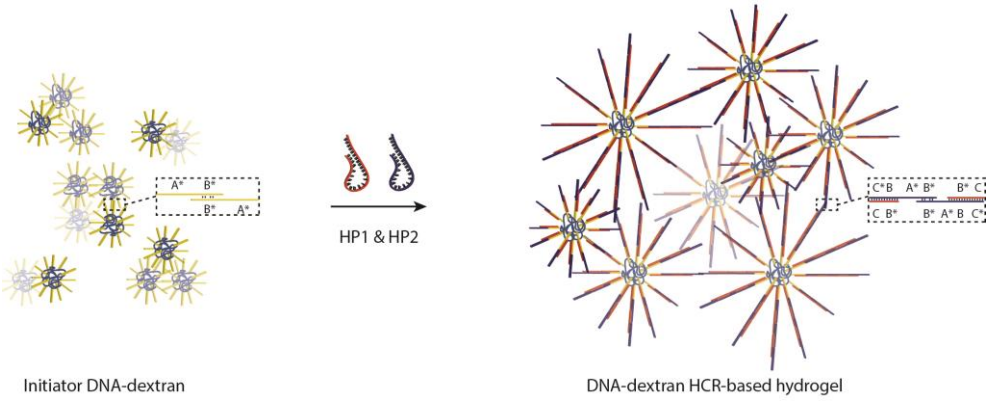

This chapter was prepared as an Original Research paper: W. E. M. Noteborn, J. A. J. Wondergem, A. Iurchenko, F. Chariyev-Prinz, D. Donato, I. K. Voets, D. Heinrich, R. E. Kieltyka

2.1 Abstract

Nucleic acid-polymer conjugates are an attractive class of materials that are endowed with tuneable and responsive character. Herein, we exploit the dynamic character of nucleic acids by the hybridization chain reaction to prepare hybrid DNA grafted covalent polymers. The cascade of sequential strand displacement reactions results in growth of the DNA grafts on a dextran polymer backbone, leading to eventual hydrogel formation with increasing concentration. Because of the growth of the DNA grafts is in a dynamic fashion, applications are envisaged where the viscoelastic properties of the material can be exploited for drug delivery or detection using viscosity as readout.

Keywords: hybridization chain reaction, graft copolymer, hydrogel, DNA, dextran.

2.2 Introduction

Nucleic acids are powerful tools for the construction of materials because of their sequence programmability and predictable dimensions.[1–3] Consequently, DNA nanotechnology has exploited its use as a structural unit for the bottom-up construction of numerous discrete two and three-dimensional architectures.[4–7] More recent developments within the field have centered on benefitting from the dynamic properties of DNA through the use of strand displacement reactions to provide reconfigurable and autonomous functions.[8–10] Strand displacement is a reaction that is fueled by the energy released in the hybridization of partial or fully complementary DNA strands through branch migration of a pre-hybridized DNA strand.[11] Catalyzed hairpin assembly (CHA),[12] entropy-driven catalysis (EDC)[13] and the hybridization chain reaction (HCR)[14,15] rely on strand displacement cascades to create multi-layered adaptable and reconfigurable DNA-based circuits,[16] autonomous DNA walkers[17,18] and amplifiers.[19,20] These techniques can be useful for a range of applications from smart therapeutics to diagnostics[9,21,22], using gel electrophoresis, fluorescence and electrical detection as readouts.

Beyond DNA nanotechnology, the inherent structural and dynamic features of nucleic acids can be an invaluable means to tailor the morphology and responsiveness of polymer materials in a programmable and tuneable fashion.[23–27] Often DNA is introduced as the water-soluble domain of a block copolymer to provide responsive micellar structures and hydrogels.[28–33] Although numerous reports have demonstrated the use of a block copolymer approach, graft copolymer architectures can provide additional handles to modify the polymer architecture through variation of grafting densities, lengths and the choice of the backbone itself.[34,35] The consequence of these structural modifications can result in a broader range of morphologies, such as worms, spheres and cylinders.[36,37]

Classically, most synthetic strategies to prepare grafted copolymers involve covalent grafting from, to, and through the polymer backbone to permanently fix the side chains[37]. On the other hand, the more recent exploration into grafting strategies based on non-covalent interactions has opened the door to a whole new range of graft copolymer materials that can be tuneable, responsive, and dynamic.[36] Non-covalent molecular recognition motifs have been used to append organic molecules and biopolymers using a non-covalent “grafting onto” approach to enable structural transitions.[38–41] Therefore, combining graft copolymers with dynamic DNA nanotechnology can yield a new class of grafted polymer hybrids that respond

through highly specific molecular interactions in a programmable and dynamic fashion with important consequences over several length scales.

Herein, we report the use of dynamic DNA nanotechnology on a hybrid dextran-DNA graft copolymer employing the hybridization chain reaction. These particles enable the autonomous growth of nucleic acid polymers off a covalent polymer backbone when supplied with two metastable hairpins (HP1 and HP2) that undergo an energetically favorable cascade of kinetically controlled strand displacement reactions (Scheme 2.1). Of important note, these hairpins can coexist stably in solution and are triggered only by the presence of the initiator DNAs. We examine the self-assembly process of the initiator DNA-dextran graft copolymer and the DNA hairpins by several molecular techniques, as well as their potential to form hydrogel materials as an output.

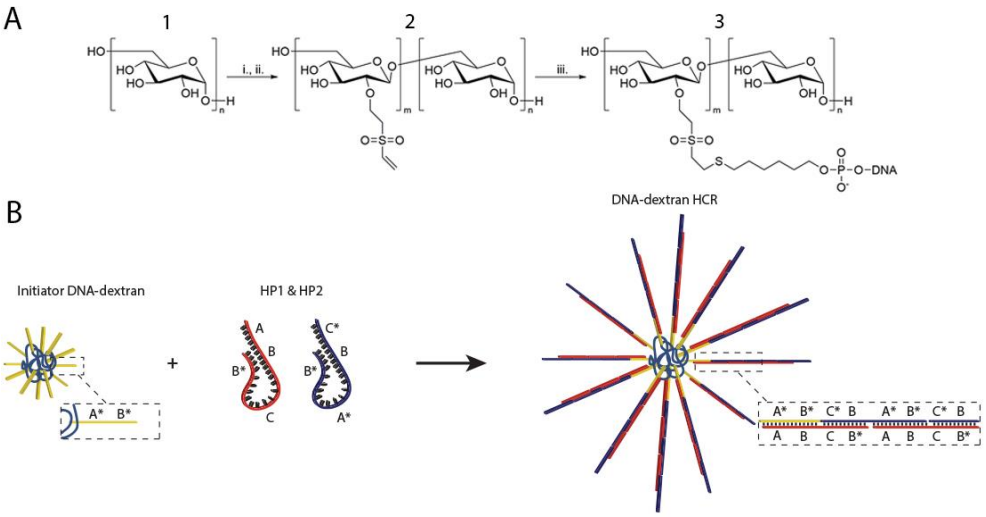

Scheme 2.1. (A) Initiator DNA-dextran graft copolymer synthesis: dextran (**1**) (Mn: 10, kDa, n_{av}: 62) was reacted with divinyl sulfone to form dextran-vinyl sulfone (dextran-VS, m_{av} = 19) (**2**). Chemoselective ligation of a thiol-modified HCR initiator single stranded DNA by a Michael addition reaction on dextran-VS (**3**). Reaction conditions: (i) 0.1 M NaOH, divinyl sulfone, (ii) 5 M HCl, (iii) 0.1 M PBS pH 8.5, using a 1 to 3 ratio of 5'-thiol-modified HCR initiator DNA with respect to the present vinyl sulfone groups. (B) Schematic representation of HCR driven non-covalent grafting from an initiator DNA-dextran graft copolymer by HP1 and HP2.

2.3 Results and discussion

To synthesize the grafted dextran copolymer with the initiator DNAs for HCR, vinyl sulfone groups were first introduced on dextran for subsequent bioconjugation with DNA. The reaction of dextran (M_n = 10 kDa) with divinyl sulfone (using 1.5 molar equivalents with respect to all hydroxyl groups) was performed under basic conditions (0.1M NaOH).[42] The sample was reacted for 0.5 minutes with thorough vortexing and immediate quenching by the addition of 5 M HCl and dialysis purification (75 % yield). By controlling the molar equivalents and reaction time, a reproducible degree of substitution of 31 % (19 hydroxyl groups functionalized per chain) was obtained as determined from ^{1}H-NMR measurements (see supporting information). Additionally, size exclusion chromatography (SEC) showed no change in dispersity (Đ ~ 1.05) or size of the vinyl sulfone substituted polymers.

In a subsequent step, dithiothreitol(DTT)-mediated deprotection of the 5'-disulfide protected initiator DNA strand was pursued to enable its conjugation to the dextran polymer by vinyl sulfone thiol-Michael addition. Excess DTT was removed by an ethyl acetate extraction to prevent a competitive reaction with the vinyl sulfone groups on dextran and the deprotected 5'-thiol DNA. The conjugation reaction was carried out immediately by mixing the freshly reduced 5'-thiol DNA with dextran-vinyl sulfone in PBS at pH 8.5 overnight under inert conditions. The formation of the DNA-dextran graft copolymer conjugate was assessed by agarose gel electrophoresis (Figure 2.1A). In comparison to the unreacted DNA (lane 1, bottom) observed as both free thiol-DNA (bottom diffuse DNA band) and dithiol species in which two thiol-DNAs reacted with each other (middle sharp DNA band), a large, slowly migrating and smeared band was observed indicative of the formation of the initiator DNA-dextran conjugate (lane 1, top). Analysis of the agarose gels by densitometry revealed that 74% of the added 5'-thiol DNAs were conjugated to dextran. Most likely, complete substitution of the vinyl sulfone groups on the polymer backbone is hindered by the high electrostatic charge and steric constraints of the DNA oligonucleotides. Gel electroelution was used to separate and remove the unreacted initiator DNA from the initiator DNA-dextran graft copolymer followed by dialysis to provide a final yield of 70 %. After purification, a 2 % agarose gel electrophoresis was performed, showing complete removal of the unreacted 5'-thiol DNA from the DNA-dextran graft copolymer (Figure 2.1A, Lane 2).

The capacity of the DNA initiator-dextran graft copolymer to trigger HCR from the polymer backbone was initially evaluated by gel electrophoresis and fluorescence

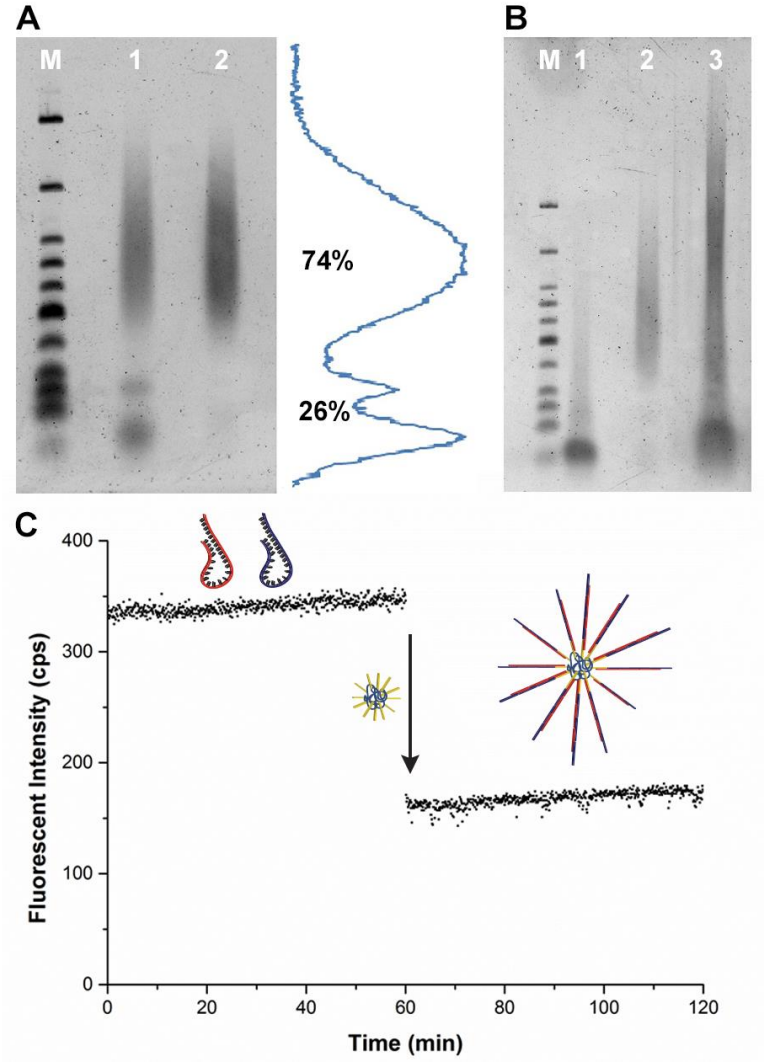

Figure 2.1. (A) Agarose gel electrophoresis (2%) of the initiator DNA-dextran graft copolymer before (Lane 1) and after purification (Lane 2). Lane M contains a low molecular weight DNA marker ranging from 25 to 766 bp. (B) Agarose gel electrophoresis (2%) showing the products of HCR after addition of the initiator DNA-dextran graft copolymer. Combination of HP1 and HP2 (Lane 1), initiator DNA-dextran graft copolymer (Lane 2), HCR of HP1 and HP2 on the initiator DNA-dextran graft copolymer (Lane 3). Lane M contains a low molecular weight DNA marker ranging from 25 to 766 bp. (C) Fluorescence time course measurement of HP1-2AP HP1 ($\lambda_{ex.}$= 303 nm, $\lambda_{em.}$= 365 nm) with HP2 and the addition at 60 minutes of the DNA-dextran initiator, triggering the hybridization chain reaction and fluorescence quenching.

spectroscopy on dilute solution phase samples to provide insight into the self-assembly process at the molecular scale. Pre-hybridized DNA hairpins (HP1, HP2) thermally annealed in 5X SSC buffer were mixed in equimolar quantities and added to the DNA initiator-dextran graft copolymer in the same buffer to start the reaction. Agarose gel electrophoresis (2%) one hour after the start of the reaction showed that addition of the folded HP1 and HP2 to the DNA-dextran graft copolymer resulted in increased retention of the polymer initiator (Figure 2.1B, Lane 3). This result would suggest growth of the DNA grafts by HCR through opening of the metastable DNA hairpins. In contrast, lower gel retention of the negative controls including the initiator DNA-dextran graft copolymer (Figure 2.1B, Lane 2) and the metastable HCR hairpins only (Figure 2.1B, Lane 1) was observed, underpinning the occurrence of the HCR reaction on the dextran polymer.

Nucleic acid fluorescence quenching experiments involving a 2-aminopurine functionalized hairpin 1 (HP1-2AP) for self-assembly further supported the findings by gel electrophoresis. 2-AP-labelled oligonucleotides are fluorescent in their single stranded form, but become rapidly quenched when hybridized. The decrease in fluorescence intensity can be directly related to hairpin polymerization in the HCR reaction. As a control, stability of the 2-AP hairpin and its polymerization without the copolymer were first examined by monitoring the fluorescence of HP1-2AP itself and when mixed with HP2, respectively. Initially, a stable fluorescence signal was recorded for both samples consistent with folded hairpins of HP1-2AP and HP2 (Figure 2.1C). After one hour, the addition of either the DNA initiator strand on its own or grafted to the dextran copolymer to the HP1-2AP and HP2 solution resulted in rapid quenching of the fluorescence signal of the 2-AP indicative of hairpin or initiator DNA-graft copolymers (Figure 2.1C) opening and polymerization of ssDNA (Figure S2.1). Collectively, these results show that DNA hairpin polymerization occurs by HCR on the DNA initiator-dextran graft copolymer.

Because of our interest in using the HCR reaction to modulate physicochemical properties of polymer materials, we examined the morphology of the DNA-graft copolymers self-assembly at the nanoscale by dynamic light scattering (DLS), small angle X-ray scattering (SAXS) and atomic force microscopy (AFM). Particle size measurements of the various components (HP1, HP2, HP1 and HP2, dextran-VS, initiator DNA-dextran and the HCR reaction mixture) as dilute solutions were examined by DLS. The individual hairpins and their combination displayed an average size of 6 nm and 8 nm, respectively (Figure 2.2A). The initiator DNA-dextran graft copolymer showed an average size on the order of 500 nm. Surprisingly, addition of

HP1 and HP2 to the initiator DNA-dextran graft copolymer resulted in the formation of micron-sized aggregates. The experimentally determined large size of the aggregates, even before addition of HP1 and HP2, suggests that clustering of the initiator DNA-polymer occurs and the resultant HCR products. A similar trend was observed by AFM for the samples prepared at room temperature except with a larger average diameter prior to the start of HCR on the initiator DNA-graft copolymer (Figure 2.2B, left, 57 ± 25 nm), and afterwards (Figure 2.2B, right, 183 ± 53 nm) with a networked structure. SAXS experiments in solution also showed aggregation of the

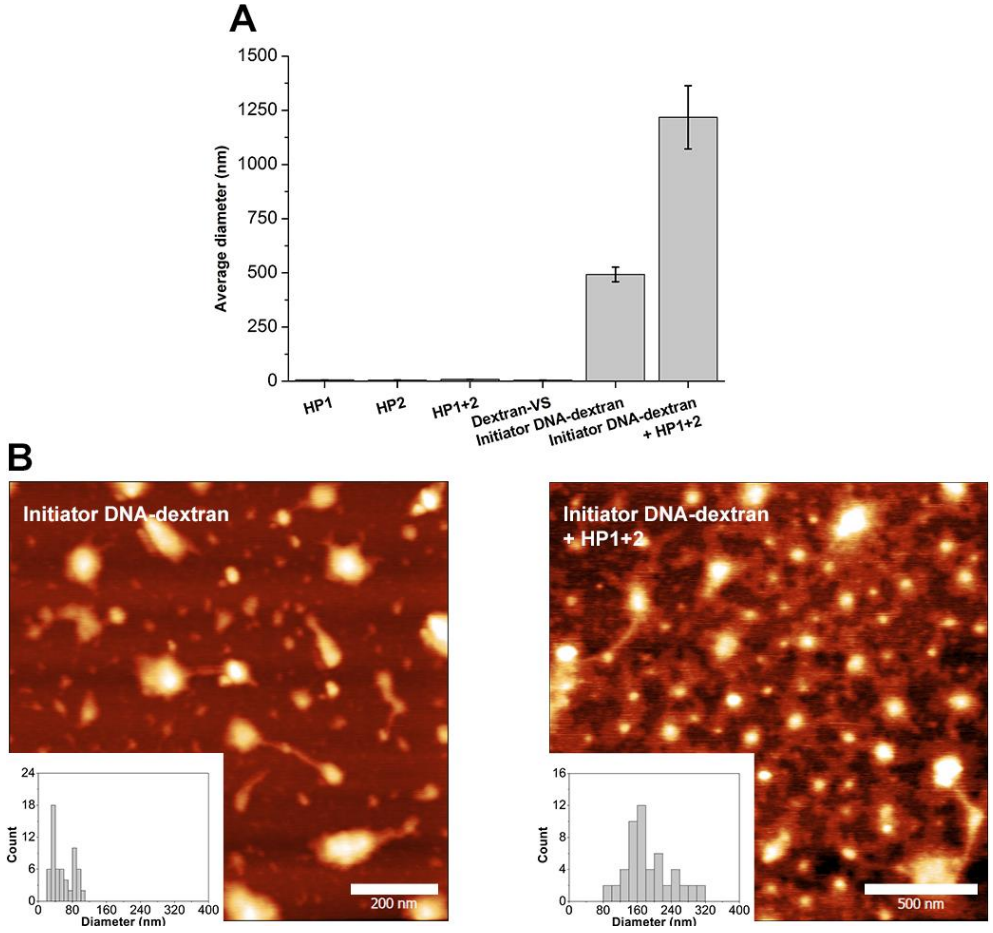

Figure 2.2. (A) Particle size distributions of native HP1, HP2, HP1 and HP2, dextran-VS, initiator DNA-dextran graft copolymer and the initiator DNA-dextran graft copolymer after HCR (left to right) by DLS. (B) Atomic force micrographs (AFM) of drop-casted native samples of initiator DNA-dextran graft copolymers before (above) and after executing HCR with HP1 and HP2 resulting in the formation of HCR DNA-dextran graft copolymers (below). Scale bars are 200 and 500 nm, respectively. Insets: histograms of DNA-dextran particle diameter.

DNA-dextran graft copolymer before and upon addition of both HP1 and HP2 at room temperature (Figure 2.3). Modeling of the HP1 and HP2 SAXS profiles with a form factor for Gaussian chains yielded a radius of gyration (R_g) of 2.5 ± 0.3 nm for HP1 and 2.3 ± 0.3 nm for HP2. Conversely, aggregates with sizes above the resolution of the instrument (π/q_{min} = 31 nm) were observed for the initiator DNA-dextran graft copolymer before and after addition of both HP1 and HP2. The experimental SAXS profile of the initiator DNA-dextran, HP1 and HP2 mixture is distinct from the theoretical SAXS profile from the sum of the 3-component mixture (Figure 2.3). This difference proves that the hairpins interact with the initiator DNA-dextran aggregates triggering a conformational change when mixed.

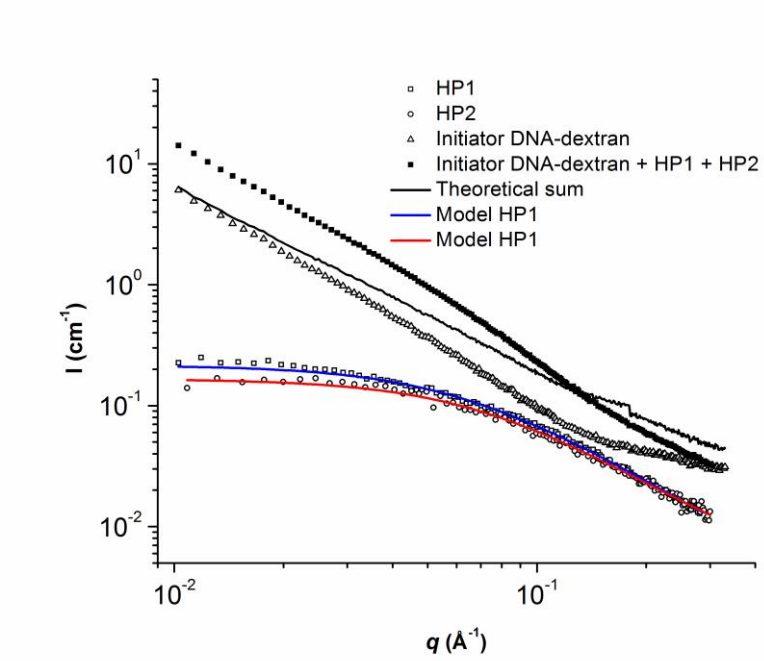

Figure 2.3. SAXS profiles of native HP1 (blue) and HP2 (red) modeled with a form factor for Gaussian chains, the initiator DNA-dextran before (black, open triangles) and after HCR (black, cubes) and a theoretical summated profile of the HCR components.

In an effort to disrupt the pre-aggregated initiator DNA-graft copolymers, the samples were heated to 60 °C before addition of HP1 and HP2 and their particle sizes were measured by DLS (Figure 2.4A). After heat treatment, initiator DNA-graft copolymers before and after subsequent hairpin addition revealed particle population with an average size of 14 nm and 66 nm, respectively, which are on par with theoretically estimated size predictions and points to the likely disruption of the

initiator DNA-graft polymer aggregates. The changes in particle diameter were further supported by AFM imaging on both 60°C and room temperature samples drop-casted on mica before and after HCR. Prior to the addition of HP1 and HP2, the 60°C sample of the initiator DNA-dextran graft copolymer showed small aggregates highly disperse in diameter (Figure 2.4B, left, 14 ± 10 nm). These spherical aggregates grew in size after addition of HP1 and HP2 with the formation of hairy protrusions (Figure 2.4B, right, 40 ± 18 nm).

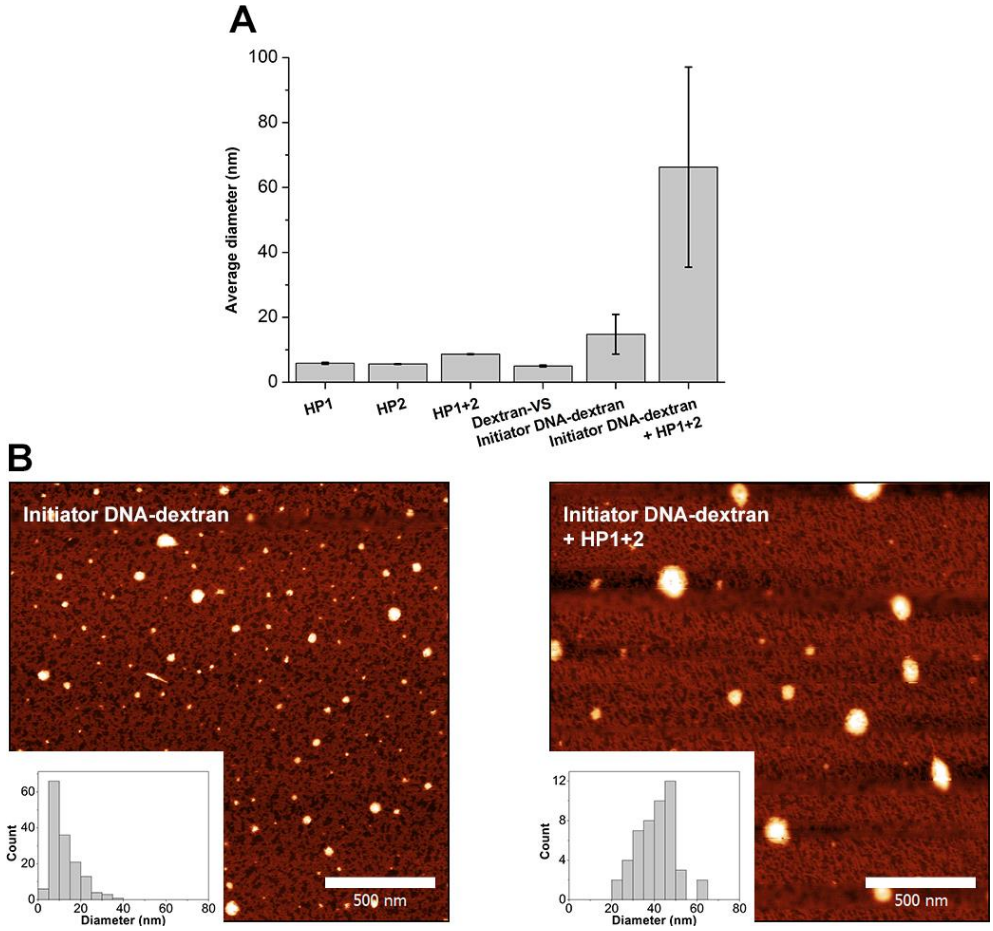

Figure 2.4. (A) Particle size distributions of heat treated HP1, HP2, HP1 and HP2, dextran-VS, initiator DNA-dextran graft copolymer and the initiator DNA-dextran graft copolymer after HCR (left to right) by DLS. (B) Atomic force micrographs (AFM) of drop-casted heat treated samples of initiator DNA-dextran graft copolymers before (above) and after executing HCR with HP1 and HP2 resulting in the formation of HCR DNA-dextran graft copolymers (below). Scale bar is 500 nm. Insets: histograms of DNA-dextran particle diameter.

To rationalize the increased aggregate sizes prior to HCR on the initiator DNA-dextran graft copolymer, in-depth analysis of the DNA sequences by NUPACK[43] was pursued. These investigations revealed weak homodimer interactions between four nucleotides in the initiator DNA strands (B*), and HP1 and HP2 (B*) once hybridized with a computed free energy of -11.09 kcal/mol. This value is in contrast to a computed free energy of -40.86 kcal/mol for each formed duplex during the HCR reaction. By careful DNA sequence evaluation, weak homodimer interactions are proposed to occur at the outset before HCR of the initiator DNA-grafted polymer and afterwards (Scheme 2.2). These computational results are in agreement with the large aggregate sizes observed solely for the initiator DNA-graft copolymer by experiment and may contribute to the greater aggregate sizes observed after HCR. However, it is unclear the extent to which each effect contributes to the final large aggregate sizes after polymerization, but it appears that both play a role in the formed products.

Finally, the potential of forming hybrid-DNA polymer materials by performing HCR on a grafted initiator DNA-polymer was probed at high polymer concentrations (1.25 – 5.0 wt%) using particle-tracking microrheology. This technique involves determining the mean squared displacement (MSD) of micrometer fluorescently labeled tracer particles subject to Brownian motion within the material over time. Whereas conventional oscillatory rheology requires large sample volumes, particle-tracking microrheology requires volumes as low as 10 µL, which is highly advantageous for the screening of physicochemical properties of DNA-based materials. Fluorescently-labeled polystyrene beads 1 µm in diameter were mixed within: a solution of HP1 and HP2 (Figure 2.5A, B, C, black tracks), initiator DNA-dextran graft copolymer lacking the HCR hairpins (red tracks) various solutions of initiator DNA-dextran graft-copolymer, to which were added to the initiator DNA-dextran copolymer (green tracks). In these experiments, a total polymer concentration of 1.25, 2.5 and 5 wt% of the DNA initiator-dextran copolymer and/or a 3-fold excess of both HP1 and HP2 were examined. For the various conditions, the bead tracks were followed over time to monitor the self-assembly process of the DNA-grafts (green tracks: 0-20 minutes, blue tracks: 20-40 minutes). The combination of the initiator DNA-dextran graft copolymer and both hairpins HP1 and HP2 showed significantly reduced Brownian motion-induced bead displacements over time in comparison to control samples. The strongest reduction of particle motion was

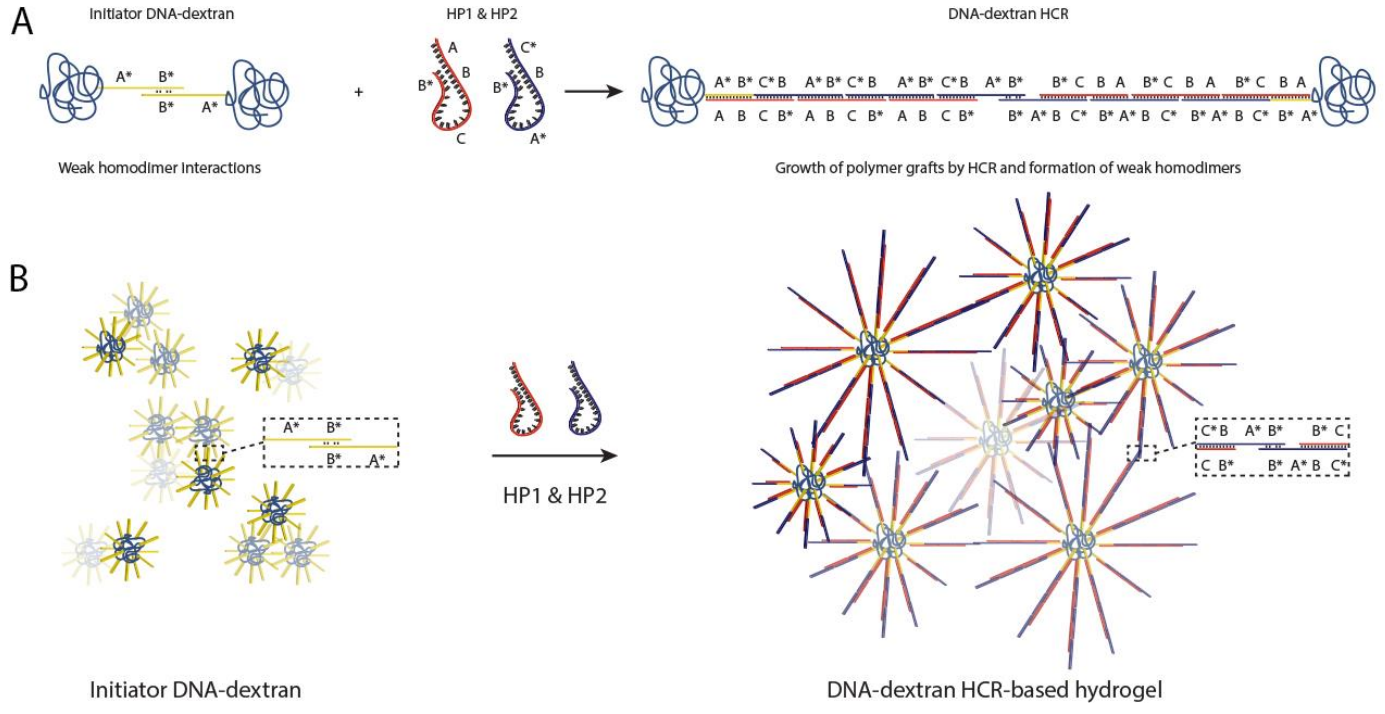

Scheme 2.2. Proposed mechanism of initiator DNA-graft copolymer self-assembly before and after HCR. (A): Initiator DNA-dextran graft copolymer bearing multiple initiator sequences can aggregate through weak homodimer interactions in domain B*. Addition of HP1 and HP2 starts the energetically favorable HCR reaction on the initiator DNA-dextran graft copolymer results in the growth of the DNA grafts. Exposed single stranded B* domains on HP1 and HP2 incorporated on the grafted supramolecular polymer can form weak homodimer interactions to form larger aggregated structures. (B) Growth mechanism of DNA grafts by HCR on the initiator DNA-dextran graft copolymer at the nanoscale. By HCR driven grafting from in a non-covalent manner using HP1 and HP2 the initial DNA-initiator graft copolymer aggregates grow in size with weak homodimer interactions facilitating further aggregation and eventual network percolation.

observed for the 5 wt% mixtures, such that axes with smaller increments for x and y displacements were required for better visualization. These particle tracks were converted into MSDs and plotted with respect to time by time-wise data segmentation (Figure 2.6A, B and C, respectively). Control samples containing only HP1 and 2 (black) or initiator DNA-dextran graft copolymer (red) displayed a linear increase in their MSDs over lag time consistent with the power law behavior of Newtonian fluids for all sample concentrations. Addition of HP1 and HP2 to the initiator DNA-dextran copolymer resulted in a decrease in the MSD values with respect to time (green: 0-20 minutes, blue: 20-40 minutes) for the 1.25 and 2.5 wt% solutions, indicative of increasingly viscous materials. For the 5.0 wt% sample, a decrease in both the MSD values as well as a slope of zero was observed on par with

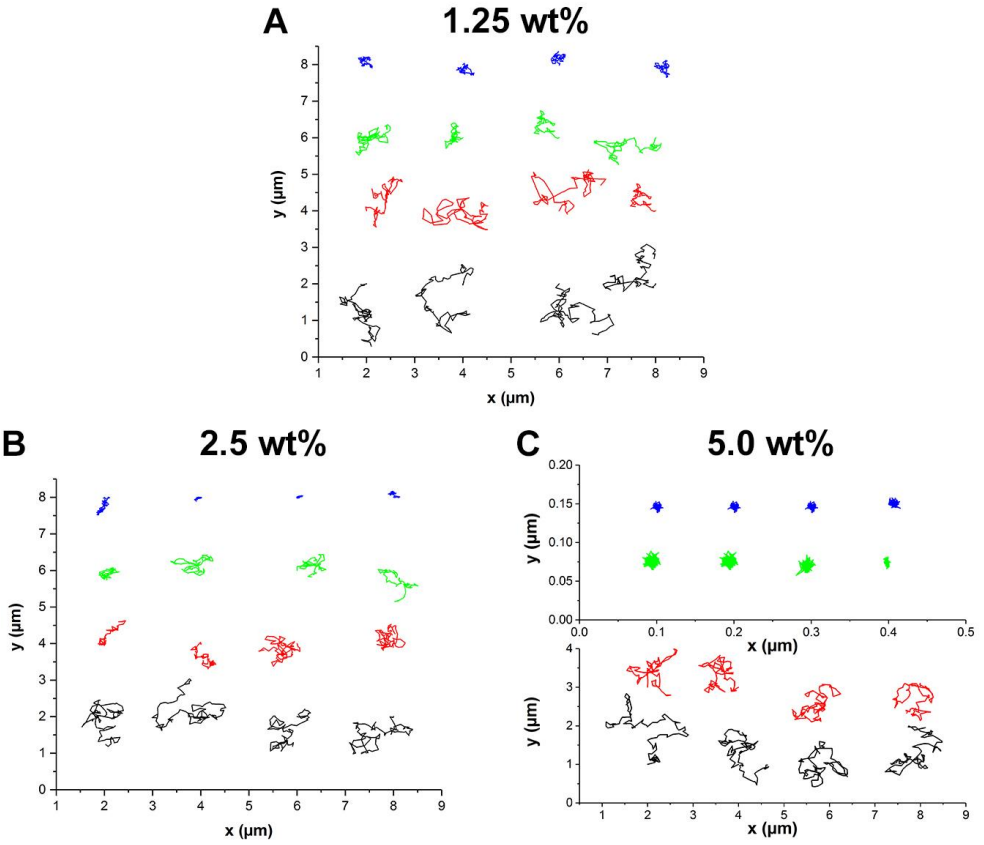

Figure 2.5. Particle tracking microrheology on 1.25, 2.5 and 5.0 wt% DNA-dextran HCR samples under various conditions. *Black*: HP1+2 only, *red*: initiator DNA-dextran only, *green*: HCR containing initiator DNA-dextran and HP1+2 0-20 minutes, *blue*: 20-40 minutes: A, B, C) Representative collections of displacement tracks for 4 beads per test condition for 1.25, 2.5 and 5.0 wt% samples, respectively.

the rapid formation of a viscoelastic solid material. As a control, performing the same HCR experiments on 2.5 wt% samples with an unconjugated initiator DNA did not result in the formation of equally viscous materials as seen in samples containing the initiator DNA-dextran graft copolymer (Figure S2.3).

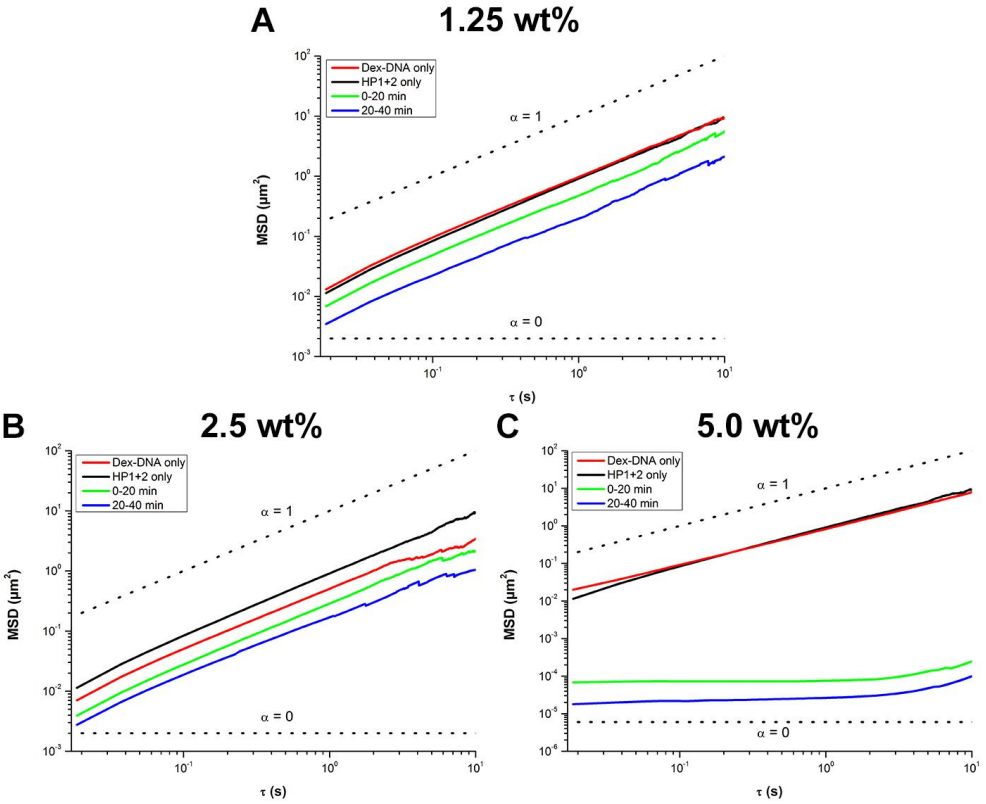

Figure 2.6. Particle tracking microrheology on 1.25, 2.5 and 5.0 wt% DNA-dextran HCR samples under various conditions. A, B, C) MSD versus lag time plots for 1.25, 2.5 and 5.0 wt% samples, respectively.

To gain further insight into the physicochemical properties of the materials, the storage (G') and loss (G") moduli were extracted from the complex modulus obtained from a numerical approximation of the Laplace transform of the MSD data. G' and G" of the various samples (1.25, 2.5 and 5 wt%, Figure 2.7A, B, C respectively) as a function of frequency were determined after 40 minutes of equilibration. As expected, for the 1.25 and 2.5 wt% samples *G*" was greater than *G*' over the entire frequency range consistent with liquid-like behavior. Conversely, for the 5 wt% *G*' was greater than *G*", synonymous with the formation of a viscoelastic material. Most likely, the growth of the DNA grafts by the HCR reaction and weak homodimer

interactions are involved in the macroscopic gel-like behavior recorded for the 5 wt% sample.

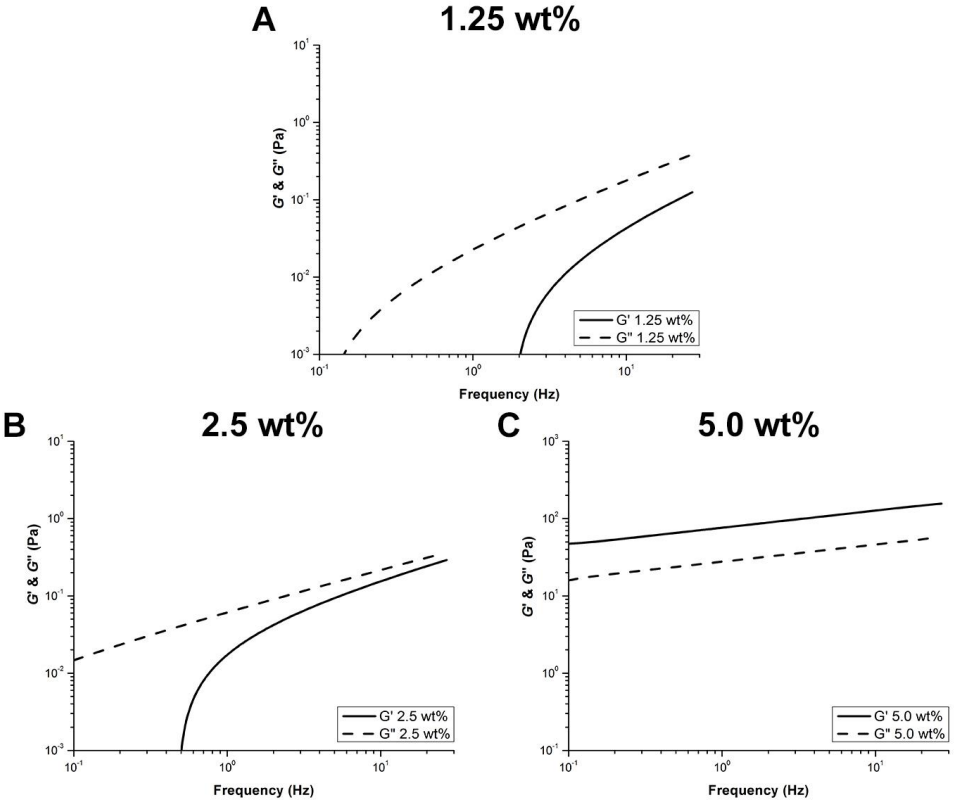

Figure 2.7. Particle tracking microrheology on 1.25, 2.5 and 5.0 wt% DNA-dextran HCR samples under various conditions. A, B, C) Rheological properties as a function of frequency for 1.25, 2.5 and 5.0 wt% samples, respectively (*solid lines*: G', *dashed lines*: G").

2.4 Conclusions

The DNA hybridization chain reaction is a hallmark example of dynamic DNA nanotechnology that can be used for sophisticated applications in detection with limits in the femtomolar range. We have shown that this technique based on DNA strand displacement can be applied on covalent polymers to drive on-demand growth of aggregate sizes with the potential to form macroscale materials depending on concentration. In combination with the advances in DNA solid phase synthesis and its continuously decreasing production costs, we envisage that implementing this technique on polymer materials opens up this area to a whole new level of structural abstraction, allowing for the future development of a wide range of responsive materials for applications in diagnostics and drug delivery, using viscosity-based changes as a readout.

2.5 References

1 McLaughlin, C. K.; Hamblin, G. D.; Sleiman, H. F. Chem. Soc. Rev. 2011, 40 (12), 5647.

2 Seeman, N. C. 2003, 421 (January), 1122.

3 Pinheiro, A. V; Han, D.; Shih, W. M.; Yan, H. Nat. Publ. Gr. 2011, 6 (12), 763.

4 Rothemund, P. W. K. Nature 2006, 440 (7082), 297.

5 Sobczak, J.-P. J.; Martin, T. G.; Gerling, T.; Dietz, H. Science 2012, 338 (6113), 1458.

6 Aldaye, F. A.; Palmer, A. L.; Sleiman, H. F. Science 2008, 321 (5897), 1795.

7 Douglas, S. M.; Bachelet, I.; Church, G. M. Science 2012, 335 (6070), 831.

8 Zhang, D. Y.; Seelig, G. Nat. Chem. 2011, 3 (2), 103.

9 Chen, Y. J.; Groves, B.; Muscat, R. A.; Seelig, G. Nat Nanotechnol 2015, 10 (9), 748.

10 Freeman, R.; Stephanopoulos, N.; Álvarez, Z.; Lewis, J. A.; Sur, S.; Serrano, C. M.; Boekhoven, J.; Lee, S. S.; Stupp, S. I. 2017, 8, 15982.

11 Zhang, D. Y.; Winfree, E. J. Am. Chem. Soc. 2009, 131 (47), 17303.

12 Li, B.; Ellington, A. D.; Chen, X. Nucleic Acids Res. 2011, 39 (16), e110.

13 Zhang, D. Y.; Turberfield, A. J.; Yurke, B.; Winfree, E. Science 2007, 318 (5853), 1121.

14 Dirks, R. M.; Pierce, N. A. Proc. Natl. Acad. Sci. U. S. A. 2004, 101 (43), 15275.

15 Choi, H. M. T.; Beck, V. a.; Pierce, N. a. ACS Nano 2014, 8, 4284.

16 Seelig, G.; Soloveichik, D.; Zhang, D. Y.; Winfree, E. Science 2006, 314 (5805), 1585.

17 Shin, J.; Pierce, N. a. J. Am. Chem. Soc. 2004, 126 (35), 10834.

18 Sherman, W. B.; Seeman, N. C. Nano Lett. 2004, 4 (7), 1203.

19 Zhang, D. Y.; Winfree, E. J. Am. Chem. Soc. 2008, 130 (42), 13921.

20 Zhang, D. Y.; Hariadi, R. F.; Choi, H. M. T.; Winfree, E. Nat. Commun. 2013, 4 (May), 1965.

21 Xu, Q.; Zhu, G.; Zhang, C. Y. Anal. Chem. 2013, 85 (14), 6915.

22 Rudchenko, M.; Taylor, S.; Pallavi, P.; Dechkovskaia, A.; Khan, S.; Butler Jr, V. P.; Rudchenko, S.; Stojanovic, M. N. Nat. Nanotechnol. 2013, 8 (8), 580.

23 Shao, Y.; Jia, H.; Cao, T.; Liu, D. Acc. Chem. Res. 2017, 50 (4), 659.

24 Serpell, C. J.; Edwardson, T. G. W.; Chidchob, P.; Carneiro, K. M. M.; Sleiman, H. F. J. Am. Chem. Soc. 2014, 136 (44), 15767.

25 Noteborn, W. E. M.; Zwagerman, D. N. H.; Talens, V. S.; Maity, C.; van der Mee, L.; Poolman, J. M.; Mytnyk, S.; van Esch, J. H.; Kros, A.; Eelkema, R.; Kieltyka, R. E. Adv. Mater. 2017, 1603769.

26 Vyborna, Y.; Vybornyi, M.; Haner, R. Chem. Commun. 2017.

27 Chen, P.; Li, C.; Liu, D.; Li, Z. Macromolecules 2012, 45 (24), 9579.

28 Wilks, T. R.; Bath, J.; de Vries, J. W.; Raymond, J. E.; Herrmann, A.; Turberfield, A. J.; O'Reilly, R. K. ACS Nano 2013, 7 (10), 8561.

29 Rodríguez-Pulido, A.; Kondrachuk, A. I.; Prusty, D. K.; Gao, J.; Loi, M. A.; Herrmann, A. Angew. Chem. Int. Ed. 2013, 52 (3), 1008.

30 Soontornworajit, B.; Zhou, J.; Shaw, M. T.; Fan, T.-H.; Wang, Y. Chem. Commun. 2010, 46 (11), 1857.

31 Kahn, J. S.; Trifonov, A.; Cecconello, A.; Guo, W.; Fan, C.; Willner, I. Nano Lett. 2015, 15 (11), 7773.

32 Liao, W.-C.; Lilienthal, S.; Kahn, J.; Riutin, M.; Sohn, Y. S.; Nechushtai, R.; Willner, I. Chem. Sci. 2017, 8, 3362.

33 Tan, X.; Lu, X.; Jia, F.; Liu, X.; Sun, Y.; Logan, J. K.; Zhang, K. J. Am. Chem. Soc. 2016, 138 (34), 10834.

34 Ohno, S.; Matyjaszewski, K. J. Polym. Sci. Part A Polym. Chem. 2006, 44 (19), 5454.

35 Lee, H. Il; Pietrasik, J.; Sheiko, S. S.; Matyjaszewski, K. Prog. Polym. Sci. 2010, 35 (1–2), 24.

36 Feng, C.; Li, Y.; Yang, D.; Hu, J.; Zhang, X.; Huang, X. Chem. Soc. Rev. 2011, 40 (3), 1282.

37 Sheiko, S. S.; Sumerlin, B. S.; Matyjaszewski, K. Progress in Polymer Science (Oxford). 2008, pp 759–785.

38 Petersen, H.; Fechner, P. M.; Martin, A. L.; Kunath, K.; Stolnik, S.; Roberts, C. J.; Fischer, D.; Davies, M. C.; Kissel, T. Bioconjug. Chem. 2002, 13 (4), 845.

39 Schubert, U. S.; Hofmeier, H. Macromol. Rapid Commun. 2002, 23 (9), 561.

40 South, C. R.; Burd, C.; Weck, M. Acc. Chem. Res. 2007, 40 (1), 63.

41 Hammond, M. R.; Li, C.; Tsitsilianisb, C.; Mezzenga, R. Soft Matter 2009, 5, 2371.

42 Yu, Y.; Chau, Y. Biomacromolecules 2012, 13 (3), 937.

43 Zadeh, J. N.; Steenberg, C. D.; Bois, J. S.; Wolfe, B. R.; Pierce, M. B.; Khan, A. R.; Dirks, R. M.; Pierce, N. A. J. Comput. Chem. 2011, 32 (1), 170.

2.6 Supporting Information

2.6.1 Materials

Ethyl acetate, tris(hydroxymethyl)aminomethane (Tris base), boric acid, sodium chloride, sodium phosphate monobasic, sodium phosphate dibasic 3-hydroxypicolinic acid, divinyl sulfone, hydrochloric acid, sodium azide, 1,4-dithiothreitol (DTT), Agarose and Nile Red were obtained from Sigma Aldrich. Ammonium citrate dibasic, sodium hydroxide and ethylenediaminetetraacetic acid (EDTA) were purchased from Fluka. Dextran (Mn: 10kDa) was obtained from Pharmacosmos (Uppsala, Sweden). Dialysis membranes were purchased from Spectrum Laboratories (Rancho Dominguez, CA, USA). DNA loading buffer and 1.0 µm TetraSpeck™ fluorescent polystyrene beads were purchased from Thermo Scientific and GelRed nucleic acid stain was obtained from Biotium. Oligonucleotides were commercially synthesized (IDT, Coralville, IA, USA). Micro-insert 4 well chambers were obtained from Ibidi. Water was deionized prior to use.

2.6.2 DNA sequences

5'-Thiol-C6 modified and unmodified oligonucleotides used in this study:

	Sequence (5' - 3')	MW (Da)
Initiator DNA-thiol	/5ThioMC6-D/AGTCTAGGATTCGGCGTGGGTTAA	7792.3
HP1	TTAACCCACGCCGAATCCTAGACTCAAAGTAGTCTAGGATTCGGCGTG	14736.6
HP2	AGTCTAGGATTCGGCGTGGGTTAACACGCCGAATCCTAGACTACTTTG	14798.6

2.6.3 Instrumentation

DNA hybridization and heating of reactions were performed on an Eppendorf Thermomixer C. Gel electrophoresis studies were performed using a 20 x 20 cm standard horizontal electrophoresis unit and the resulting agarose gels were scanned using a Molecular Imager Gel Doc XR System. Measurement of DNA concentration was recorded on a Cary 300 UV-Vis spectrophotometer equipped with a Peltier

thermostatted cell holder, using 10 mm path length quartz cuvettes. Matrix-assisted laser desorption ionization–time-of-flight (MALDI-TOF)-MS spectra were acquired on a Bruker microflex LRF mass spectrometer in linear positive-ion mode using 3-hydroxypicolinic acid as a matrix on a ground steel target plate. Nuclear magnetic resonance spectra (1HNMR, 300 MHz) were recorded on a Bruker DPX300 with chemical shifts reported to the residual solvent peak (D2O). Dynamic light scattering (DLS) experiments were performed on a Malvern Zetasizer Nano S using plastic cuvettes with a 10 mm path length and measurements were taken at an angle of 173°. Size exclusion chromatography experiments were performed with two detectors consisting of an interferometric RI-detector (Optilab DSP, Wyatt Technology) in line with a multi angle light scattering detector (Dawn-DSP-F, Wyatt Technology). Fluorescence data was obtained by using a fluorescent microplate reader TECAN infinite M100Pro (Switzerland). Excitation and emission wavelengths for 2-AP fluorescence quenching experiments were 303 nm and 365 nm, respectively, recorded with 4-nm bandwidths. Microrheology experiments were performed on a Nikon Eclipse Ti-E inverted microscope equipped with a confocal spinning disk unit (CSU-X1) operated at 10,000 rpm (Yokogawa, Japan) using a 100x Plan Fluor Lens (Nikon, Japan) and excited with a 488 solid state diode laser (Coherent, U.S.A.) by tracking 1.0 µm fluorescently labeled TetraSpeck polystyrene beads. Images were captured every 0.0186 seconds for 50000 frames by an Andor iXon Ultra 897 High Speed EM-CCD camera (Andor Technology, Northern Ireland). AFM micrographs were acquired in tapping mode imaging on a JPK Nanowizard Ultra AFM (JPK Instruments, Germany), using 70 kHz resonance frequency, 2 N/m force constant silicon cantilever tips. Small angle X-ray scattering measurements were performed on a SAXSLAB GANESHA 300 XL SAXS system, which comprises a GeniX 3D Cu Ultra Low Divergence micro focus sealed tube source producing X-rays with a wavelength λ = 1.54 Å at a flux of 1x108 ph/s and a Pilatus 300K silicon pixel detector with 487 x 619 pixels of 172 µm x 172 µm in size placed at two sample-to-detector distances of 713 and 1513 mm respectively to access a q-range of $0.01 \leq q \leq 0.3$ Å-1 with $q = 4\pi/\lambda(\sin\theta/2)$. Silver behenate was used for calibration of the beam centre and the q range. The samples were filled at room temperature into the sample holder, being 2 mm quartz capillaries (Hilgenberg Gmbh, Germany) held in a metal block. The two-dimensional SAXS patterns were brought to an absolute intensity scale using the calibrated detector response function, known sample-to-detector distance, measured incident and transmitted beam intensities, and azimuthally averaged to obtain one dimensional SAXS profiles. The one-dimensional scattering curves were corrected for scattering of the solvent and quartz cell. Modeling of the scattering profiles was performed in the

software package SasView (http://www.sasview.org/) employing a form factor model for Gaussian polymer chains.

2.6.4 Synthetic routes

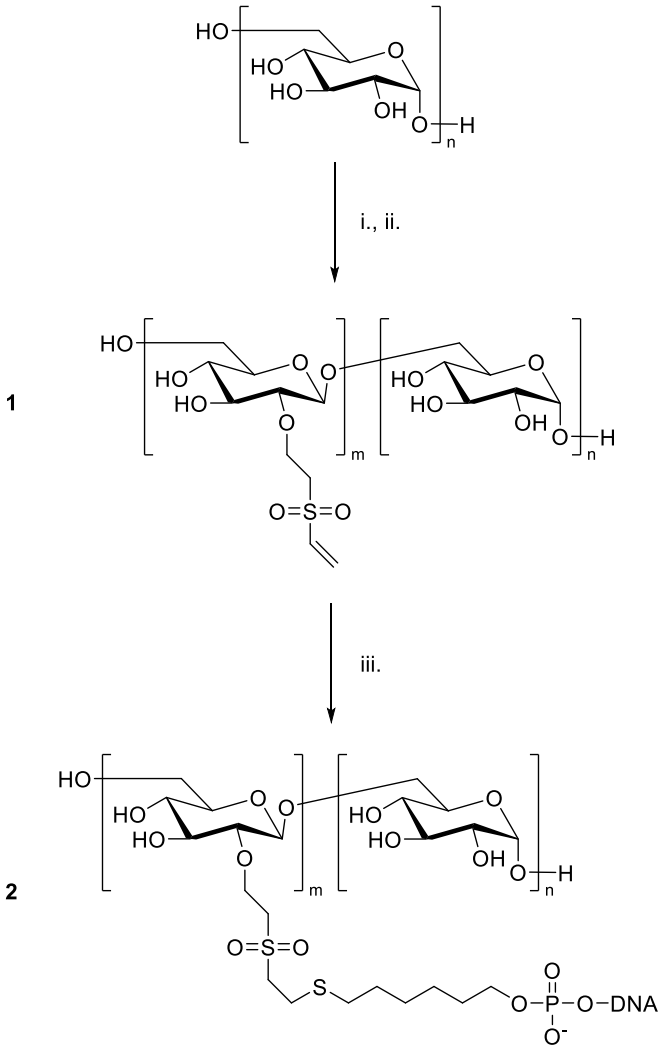

Scheme S1: Synthetic scheme for the preparation of dextran-VS and initiator DNA-dextran graft copolymer conjugates: i.) divinyl sulfone, 0.1 M NaOH, vortex, rt, 1 min, ii.) 5.0 M HCl, iii.) 5'-thiol initiator DNA, PBS 1X (pH 8.5), 37 °C, 24 h.

2.6.5 Synthesis of dextran-VS (1):

Dextran (M_n: 10.0 kDa, 0.5 g, 0.05 mmol) was dissolved in 0.1 M NaOH (5.0 mL), and to this was added divinyl sulfone (3.27 mL, 32.6 mmol) while vigorously shaking on a vortex. After 1 minute, the reaction was quenched by adjusting the pH of the reaction to pH 5.0 using 5.0 M HCl. The reaction mixture was then dialyzed for 24 hours in a dialysis bag (MWCO: 1.0 kDa) to remove excess divinyl sulfone. Afterwards, the dialyzed reaction mixture was lyophilized to provide the product as a white solid. ^{1}H-NMR (δ_H[ppm], D_2O, 300 MHz): 6.89-7.04 (m, 19H), 6.45-6.50 (d, 19H), 6.35-6.38 (d, 19H), 4.98-5.30 (m, 62H, anomeric proton), 3.30-4.10 (m, glucose units). The degree of substitution is defined using the ratio: (V / D * 100%), in which V is the integral of the vinyl sulfone protons at 6.89-7.04 ppm and D the integral of the anomeric dextran protons at 4.98-5.30 ppm as obtained from the ^{1}H-NMR spectra (19 out of 62 dextran monomers were functionalized, 31% substituted).

2.6.6 Synthesis of initiator DNA-dextran graft copolymer (2):

5'-Disulfide-protected initiator DNA oligonucleotide (1.0 mg, 130 nmol) was dissolved in phosphate buffer (200 µL, 0.1 M pH 8.0) and was reduced by adding DTT (12.0 mg, 78 µmol). The deprotection reaction was incubated for 1 hour under a nitrogen atmosphere to prevent re-oxidation at 37°C while shaking. Afterwards, DTT was removed from the reaction mixture by extraction with ethyl acetate 3 times (800 µL) and discarded. Completion of the oligonucleotide deprotection reaction was evaluated using MALDI-TOF-MS. The freshly deprotected 5'-thiol ssDNA initiator (200 µL, 130 nmol) was then added to a solution of dextran-VS (18.5 nmol, 0.19 mg) dissolved in phosphate buffer (50 µL, 0.5 M pH 8.5) and allowed to react for 24 hours while shaking at 37°C. DNA loading buffer (50 µL) was added to the crude reaction mixture. From this mixture, an aliquot with a DNA content of 500 ng was loaded in a 0.5 cm wide gel slot on a 3% agarose gel, serving as reference sample. The rest of the reaction mixture was loaded into a 10 cm wide gel slot of the same 3% agarose gel for purification. The reference band was then cut out of the gel, stained using GelRed and imaged to determine the location of the product on gel. The part of the gel containing the reaction product was then cut in pieces and loaded into a dialysis bag for electroelution of the product (1X TBE, 150 V, 3 h). The solution containing the product was the dialyzed overnight and lyophilized to obtain the initiator DNA-dextran graft

copolymer conjugate as a white powder. Conjugation and purification were checked using 2% agarose gel electrophoresis.

2.6.7 Gel electrophoresis

Agarose gel electrophoresis (2 wt%) was carried out under non-denaturing conditions using 1X TBE buffer to monitor dextran functionalization with DNA and oligonucleotide hybridization to the DNA-grafts on the dextran copolymer. For all hydrogel and intermediate stage samples, gel aliquots containing 500 ng DNA (calculated from the concentration of DNA inside the reaction volume) were prepared by dilution of the gel in water and mixed with DNA-loading buffer. The corresponding electrophoretic mobility was analyzed on gel.

2.6.8 2-AP fluorescence quenching

Stock solutions of HP1-2AP and HP2 (both 600 nM) were prepared in 5×SSC buffer, and were heated to 95 ˚C for 2 minutes and allowed to cool to room temperature for 1 hour before use. For each experiment, HP1-2AP (250 µL) was mixed with HP2 (250 µL) or with 5×SSC buffer (250 µL) in the case of the HP1-2AP only control sample. These prepared hairpin solutions were incubated at room temperature for 24 hours before the measurement. The initial fluorescence 2-AP signal was recorded after pipetting the sample into the well to obtain a stable fluorescence baseline (HP1-2AP only and HP1-2AP + HP2). After one hour, data acquisition was paused for 1 minute and Initiator DNA-dextran graft copolymer (20 µL, 200 nM) or unconjugated initiator-DNA was added prior to continuing. In both cases, addition of the initiator DNA-dextran graft copolymer or unconjugated initiator-DNA resulted in equal fluorescent quenching suggesting the HCR reaction is working on both DNA-dextran graft copolymer and DNA only substrates in a similar fashion.

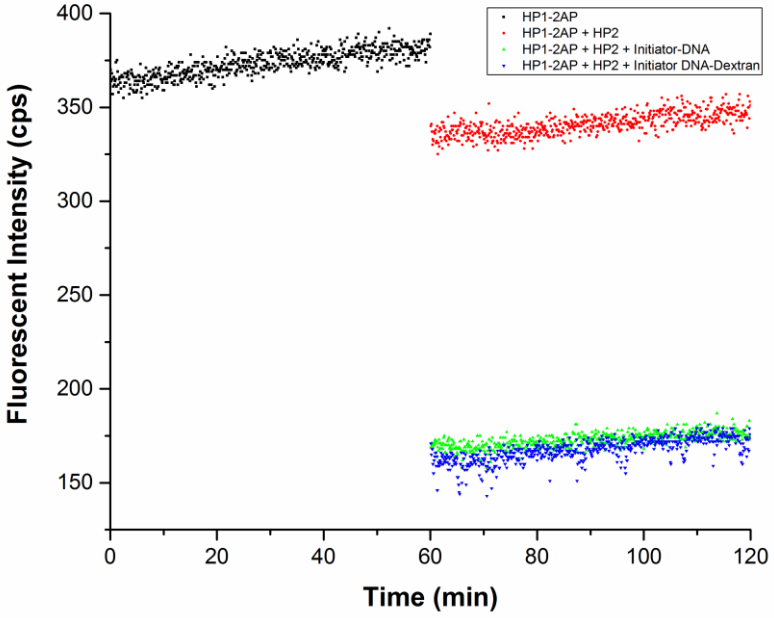

Figure S2.1. Control fluorescence quenching assays with a HP1-2AP with respect to time. Addition of HP2 (*red dots*) leads to a small drop in fluorescent intensity, suggestive of a minor interaction between the HP1and HP2. Addition of unconjugated initiator DNA (*green dots*) results in a similar drop in intensity as observed with initiator DNA-dextran graft copolymers (*blue dots*). This result suggests that the HCR reaction functions in a similar manner on both initiator DNA substrates (DNA and graft copolymer).

2.6.9 Dynamic light scattering

Dynamic light scattering (DLS) measurements were performed on 200 µL solutions of HP1, HP2, HP1 and HP2, dextran-VS, initiator DNA-dextran and the initiator DNA-dextran graft copolymer with and without performing heat treatment (60 °C). Scattered light intensities and corresponding particle sizes of all samples were measured at a 173° angle in a polystyrene cuvette at 25°C. All samples were measured in triplicate.

2.6.10 Dynamic light scattering

Initiator DNA-dextran graft copolymer conjugates (stock solution concentration: 140 µM), and HP1 and HP2 (stock solution concentration: 500 µM each) were individually dissolved in 5x SSC buffer. The initiator DNA-dextran was either used directly from storage at room temperature or thermally denatured at 60 °C for 10 minutes before performing HCR. HP1 and HP2 were heated to 95 °C for 5 minutes, after which they were allowed to cool to room temperature over one hour. The Initiator DNA-dextran graft copolymer (2.5 µL), HP1 (2.5µL) and HP2 (2.5 µL) were taken from stock solutions and mixed in 5xSSC buffer (total volume 250 µL) at room temperature for one hour. Freshly cleaved mica was incubated for 5 minutes with a 0.01 wt% solution of Poly-L-Lysine and rinsed with water two times. Afterwards, 25 µL of the HCR reaction mixture was drop-casted on the freshly coated mica and incubated for 10 minutes. The excess sample was then blotted away using filter paper and the mica surface rinsed twice with water and the excess liquid was removed. The sample was allowed to dry overnight before imaging in tapping mode by AFM.

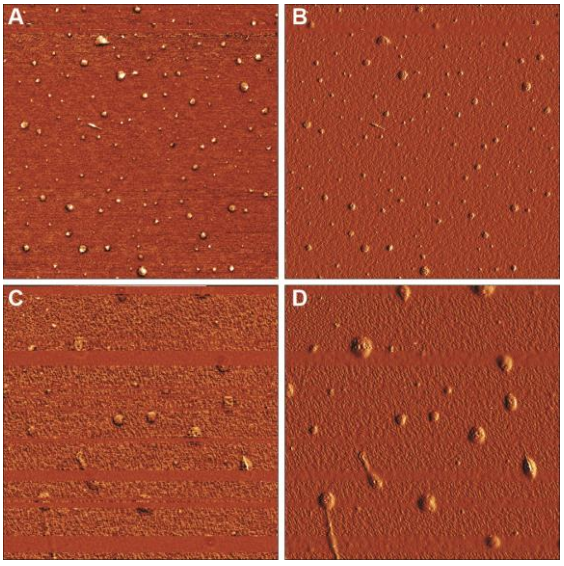

Figure S2.2. Atomic force micrographs of heat treated initiator DNA-dextran graft copolymer (A: phase, B: amplitude) and after the addition of HP1 and HP2 (C: phase, D: amplitude). Image size is 2 x 2 µm.

2.6.11 Particle-tracking microrheology

Freshly prepared samples were made by mixing the initiator DNA-dextran graft copolymer with a 3-fold excess of HP1 and HP2 and fluorescently labeled beads (TetraSpeck 1 μm polystyrene beads) to result in a final concentrations of 1.25, 2.5 and 5.0 wt% in a total volume of 11 μL. The mixtures were pipetted into an Ibidi Micro-insert 4-well chamber for fluorescent microscopy imaging of particle displacement. After image acquisition, the fluorescence signals of the beads were tracked by a center-of-mass particle tracking algorithm.[1] The algorithm is implemented in Python, named TrackPy and available online.[2] Bead trajectories were then manually checked for tracking errors and inconsistencies. Tracks for the 5.0 wt% DNA-hairpin experiment were drift corrected using a forward-rolling ensemble mean drift of 10 frames. Tracks in Figure 2 were randomly selected as an example for bead movement inside the gels. To compute the mean squared displacements (MSDs) and viscoelastic properties of the various samples, bead trajectories were processed using custom made MATLAB routines. MSDs were determined for individual trajectories and then averaged to determine the various ensemble average MSDs as a function of time and type of experiment. A cut-off of 100 data points per trajectory was used as a criterion for the inclusion of the trajectory MSD data into the ensemble average, and this criterion was re-evaluated per lag-time point. The viscoelastic curves, i.e. the storage (*G'*) and loss (*G"*) modulus, were calculated using a well-established computational scheme.[3,4] First, the ensemble averaged MSDs are calculated. Then, a numerical approximation of the Laplace transform is used to compute the complex viscoelastic modulus.[5] The exact temperature used to calculate the viscoelastic modulus was estimated using water calibrations for appropriate durations of the measurement. The viscoelastic modulus is fit to a suitable functional form (fourth-order polynomial) and then analytically continued. Finally, *G'* and *G"* are approximated by taking the real and imaginary parts of the analytical continuation.

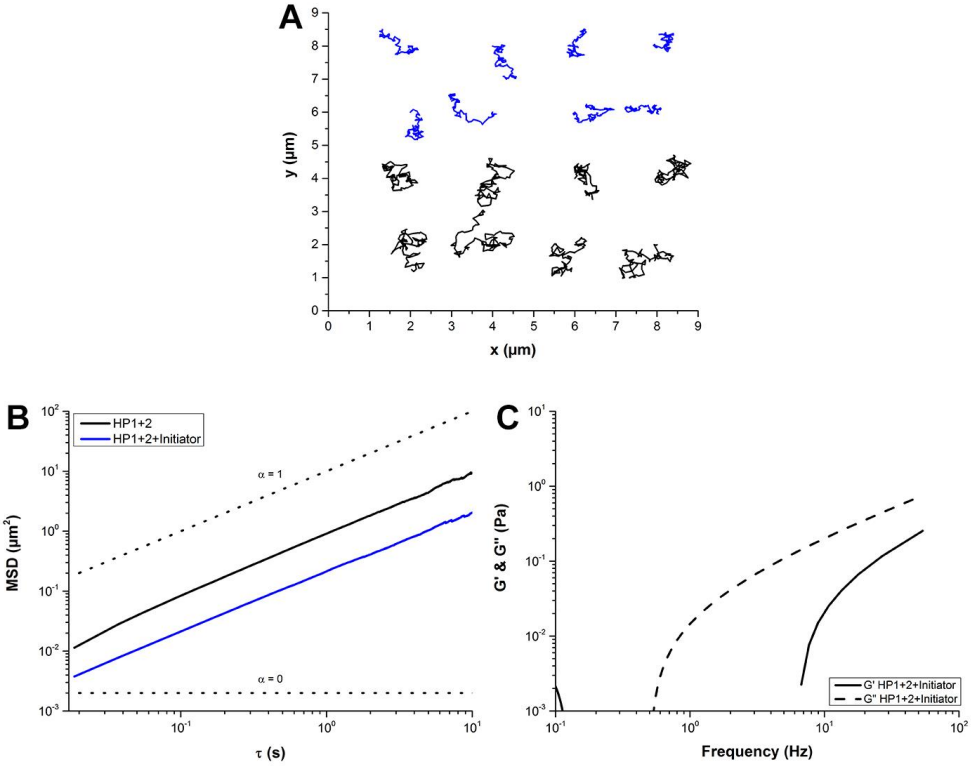

Figure S2.3. Particle tracking microrheology on 2.5 wt% unconjugated initiator DNA mixed with HP1 and HP2. A: representative collection of bead tracks (*black*: HP1+2 only, *blue*: HP1+2+initiator), B: Plot of MSD with respect to lag time, C: Rheological properties as a function of frequency.

2.6.12 References

1 Crocker, J.; Grier, D. *J. Colloid Interface Sci.* **1996**, *179* (1), 298.

2 Allan, D.; Caswell, T.; Keim, N.; van der Wel, C. August 2016,.

3 Mason, T. G.; Weitz, D. A. *Phys. Rev. Lett.* **1995**, *74* (7), 1250.

4 Mason, T. G.; Gang, H.; Weitz, D. A. *J. Mol. Struct.* **1996**, *383* (1–3), 81.

5 Hasnain, I. A.; Donald, A. M. *Phys. Rev. E* **2005**, *73* (3), 5.